Acta Biochim Biophys Sin 2013, 45: 570–577 | © The Author 2013. Published by ABBS Editorial Office in association with Oxford University Press on behalf of the Institute of Biochemistry and Cell Biology, Shanghai Institutes for Biological Sciences, Chinese Academy of Sciences. DOI: 10.1093/abbs/gmt044.
Advance Access Publication 6 June 2013

Original Article

Amyloid-β peptide (1–42) aggregation induced by copper ions under acidic conditions

Yannan Bin[2], Xia Li[1,2], Yonghui He[2], Shu Chen[1,2*], and Juan Xiang[2,3]

[1]Key Laboratory of Theoretical Chemistry and Molecular Simulation of Ministry of Education of China, School of Chemistry and Chemical Engineering, Hunan University of Science and Technology, Xiangtan 411201, China
[2]Institute of Surface Analysis and Biosensing, College of Chemistry and Chemical Engineering, Central South University, Changsha 410083, China
[3]Key Laboratory of Resources Chemistry of Nonferrous Metals, Ministry of Education, Central South University, Changsha 410083, China
*Correspondence address. Tel: +86-731-58290045; Fax: +86-731-58372324; E-mail: chenshumail@gmail.com

It is well known that the aggregation of amyloid-β peptide (Aβ) induced by Cu^{2+} is related to incubation time, solution pH, and temperature. In this work, the aggregation of $Aβ_{1-42}$ in the presence of Cu^{2+} under acidic conditions was studied at different incubation time and temperature (e.g. 25 and 37°C). Incubation temperature, pH, and the presence of Cu^{2+} in Aβ solution were confirmed to alter the morphology of aggregation (fibrils or amorphous aggregates), and the morphology is pivotal for Aβ neurotoxicity and Alzheimer disease (AD) development. The results of atomic force microscopy (AFM) indicated that the formation of Aβ fibrous morphology is preferred at lower pH, but Cu^{2+} induced the formation of amorphous aggregates. The aggregation rate of Aβ was increased with the elevation of temperature. These results were further confirmed by fluorescence spectroscopy and circular dichroism spectroscopy and it was found that the formation of β-sheet structure was inhibited by Cu^{2+} binding to Aβ. The result was consistent with AFM observation and the fibrillation process was restrained. We believe that the local charge state in hydrophilic domain of Aβ may play a dominant role in the aggregate morphology due to the strong steric hindrance. This research will be valuable for understanding of Aβ toxicity in AD.

Keywords amyloid-β peptide; copper ions; atomic force microscopy; acidic pH; morphology

Received: December 4, 2012 Accepted: February 19, 2013

Introduction

Alzheimer's disease (AD) is a progressive neurodegenerative disease characterized by abnormal amyloid accumulation in senile plaques as well as in the walls of cortical and leptomeningeal vessels of afflicted brains [1,2]. The major protein component of amyloid deposits is amyloid-β peptide (Aβ), a small peptide composed of 39–43 amino acids [2]. Studies have demonstrated that Aβ in the form of amyloid-like β-sheet structures is neurotoxic [3–5]. Extrinsic environmental factors such as peptide concentration, pH, metal ions, temperature, ionic strength, membrane-like surfaces, and solvent hydrophobicity are found to affect the proportion of Aβ secondary structures (random coil, α-helix, and β-sheet structures) [6–8]. The proportion of secondary structure is related to the morphology of Aβ, and the morphology is pivotal for the Aβ neurotoxicity and the development of AD [9,10].

Senile plaques in the neocortical region of the brain of AD patients contain up to millimolar amounts of Cu^{2+}, Zn^{2+}, and Fe^{3+} [11], and the altered H^{+} homeostasis in AD results in the decrease of local pH to 5.4 [12]. Hence, more studies focused on the influence of metal ions and pH on the aggregation and toxicity of Aβ [11,13]. pH is one of major factors to determine the aggregation rates and fibril morphologies of Aβ [13,14]. For example, Aβ is mostly unstructured in acidic aqueous solutions and exists in the form of α-helical in membrane-mimic environments such as trifluoroethanol (TFE) [15], and forms an aggregated β-sheet structure in water alone or water with TFE. The protonation states of the ionizable side-chain groups are important in β-amyloidosis. However, the effects of metal ions on Aβ aggregation reported so far are conflicting. For example, Atwood *et al.* [16] reported that copper ions accelerates Aβ aggregation, whereas Yoshiike *et al.* [17] and Raman *et al.* [18] suggested that Aβ aggregation is inhibited by these metal ions. Thus, the effects of Cu^{2+} on Aβ aggregation rate and morphology as well as structure of Aβ aggregates remain unclear. Disordered extrinsic (environmental) factors are believed to be responsible for the present situation. Therefore, the factors known to affect Aβ aggregation, such as pH and temperature, need to be taken into account systematically for clarifying the general and specific effects of Aβ/Cu^{2+} complexes on AD pathogenesis.

A deep understanding of the effect of Cu^{2+} on Aβ aggregation is necessarily required as a basis for studying the mechanisms of Aβ toxicity [19]. Atwood *et al.* [16] reported

that Aβ aggregation is accelerated by Cu^{2+}-induced effect at pH 6.0–7.0. Zhou's group [20] has shown that the presence of Cu^{2+} promotes the formation of amorphous $A\beta_{1-42}$ aggregate greatly at pH 7.4 and 6.6, and the competition between amorphous and fibrous aggregation pathways. In the present work, we studied the aggregation of $A\beta_{1-42}$ in the presence of Cu^{2+} under lower pH and compared the results with those observed in the absence of Cu^{2+}. The local charge states of the peptide were considered in the context of Aβ conformational changes, as well as the kinetics of β-sheet formation and stacking. The results of fluorescence spectroscopy and circular dichroism (CD) spectroscopy indicated that the presence of Cu^{2+} decreased the formation of Aβ fibrillation under lower pH by inhibiting β-sheet structure formation.

Materials and Methods

Materials

Lyophilized $A\beta_{1-42}$ (97% pure) was purchased from American Peptide Company (Sunnyvale, USA). All other chemicals were obtained from Sigma-Aldrich (St Louis, USA), unless otherwise stated. To ensure no substantial aggregation occurred and get rid of any aggregate in the solution, Aβ samples were routinely prepared using our previously described method [21]. The Aβ solution was freshly prepared by dissolving sample in 5 mM NaOH to a final concentration of 0.25 mM. The solution was sonicated for 1 min and kept at room temperature for 10 min to completely dissolve the sample. Centrifugation at 13,000 rpm for 30 min at 4°C was performed to remove any aggregate formed in the solution. The supernatant was used as stock solution. Prior to each experiment, aliquots of 0.25 mM stock solution were diluted with 10 mM phosphate buffer (pH 4.0 or 5.0) to 25 μM. All aqueous solutions were prepared using deionized water with a resistivity of 18.2 MΩ cm collected from a Millipore Simplicity 185 System (Millipore Co., Billerica, USA).

Atomic force microscopy

Atomic force microscopy (AFM) images were obtained using a PicoScan SPM microscope (Molecular Imaging, Phoenix, USA) equipped with a magnetic AC (MAC) mode, in which the magnetically coated probe oscillates near its resonant frequency under an alternating magnetic field. Aliquots of Aβ or Aβ/Cu^{2+} (10 μl) were collected at a predetermined incubation time, dropped onto the freshly cleaved mica, and kept in contact with the surface in a humid chamber for 15 min. Afterwards, the slides were rinsed with water gently to remove salt and unattached Aβ or Aβ/Cu^{2+}, and then dried with N_2.

Thioflavin T fluorescence assay

Steady-state thioflavin T (ThT) fluorescence of Aβ or Aβ/Cu^{2+} was measured at room temperature with a Hitachi F-2500 fluorescence spectrophotometer (Hitachi High-Technologies Co., Tokyo, Japan). ThT is a fluorescent dye that specifically binds with the β-sheet of amyloid structures [22]. The fluorescent product has a characteristic emission at 485 nm and maximum excitation at 466 nm.

Circular dichroism measurement

The effect of Cu^{2+} on the secondary structures of Aβ at different pH or temperature was assessed using a Jasco J-815 CD spectrometer (JASCO Inc., Tokyo, Japan). The measurements were performed in a cuvette cell with 1 mm path length. Scans were made from 270 to 190 nm. The following parameters were used: 500 nm/min scanning speed, 0.05 nm data acquisition interval, five accumulations, and 1 nm bandwidth.

Zeta potential measurement

Experiments were carried out in the folded capillary cell with a Zetasizer Nano ZS instrument (Malvern Instruments, Southborough, UK). During aggregation, the potential was found to be stable within a few minutes and then changed with time. All potentials were stable potentials measured in the first few minutes.

Results

The morphology of Aβ aggregates in the presence of Cu^{2+} at a pH close to the isoelectric point of Aβ

The morphology of Aβ aggregates in the absence or presence of Cu^{2+} was studied at pH 5, which is close to the isoelectric point of Aβ (pI 5.5) [23]. A few Aβ oligomers appeared at the beginning of the incubation in Aβ solutions with Cu^{2+} [**Fig. 1(E)**] or without [**Fig. 1(A)**] Cu^{2+}. After 12 h incubation at 25°C, a large number of amorphous aggregates formed in solutions [**Fig. 1(B,F)**]. As time elapsed, larger amorphous aggregates emerged in the absence of Cu^{2+} [**Fig. 1(D)**]. These results were consistent with the findings of Wood *et al.* [24] that amorphous aggregates were formed by incubating $A\beta_{1-40}$ at pH 5.8. A similar aggregate morphology was also observed in the Cu^{2+}-containing Aβ solution [**Fig. 1(H)**]. No difference was found between the morphologies of Aβ aggregates formed in the presence or in the absence of Cu^{2+} at pH 5.0, which is close to the isoelectric point of Aβ.

Lower pH favors the formation of Aβ fibril

To determine the effect of pH on the formation of amorphous aggregates, the aggregation process of Aβ in the presence or absence of Cu^{2+} was conducted at lower pH. The morphologies of Aβ aggregates formed in the presence or

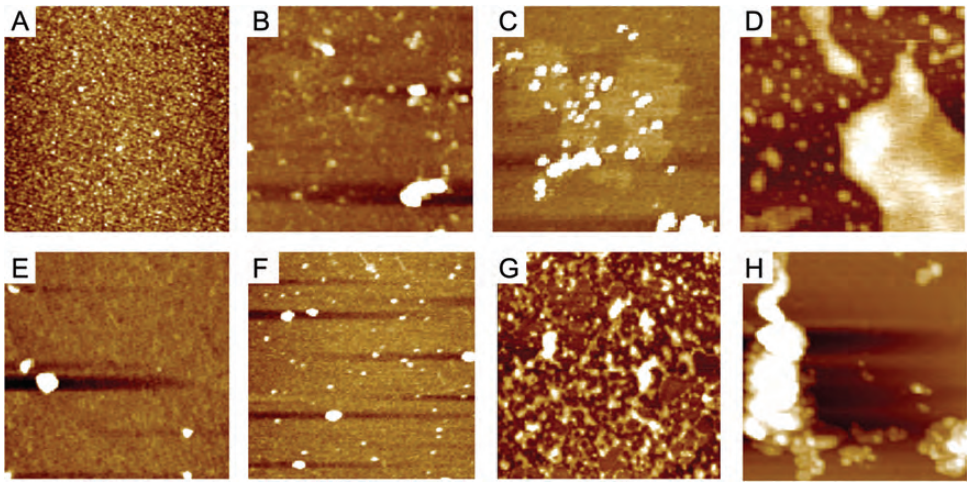

Figure 1 AFM images of Aβ solutions in the presence or absence of Cu^{2+} incubated at pH 5 and 25°C for different time Aβ solutions in the absence of Cu^{2+} incubated for 0 h (A), 12 h (B), 48 h (C), and 168 h (D), as well as in the presence of Cu^{2+} incubated for 0 h (E), 12 h (F), 48 h (G), and 168 h (H). The concentration of Aβ or Cu^{2+} was 25 μM. The scan area was 1 × 1 μm^2.

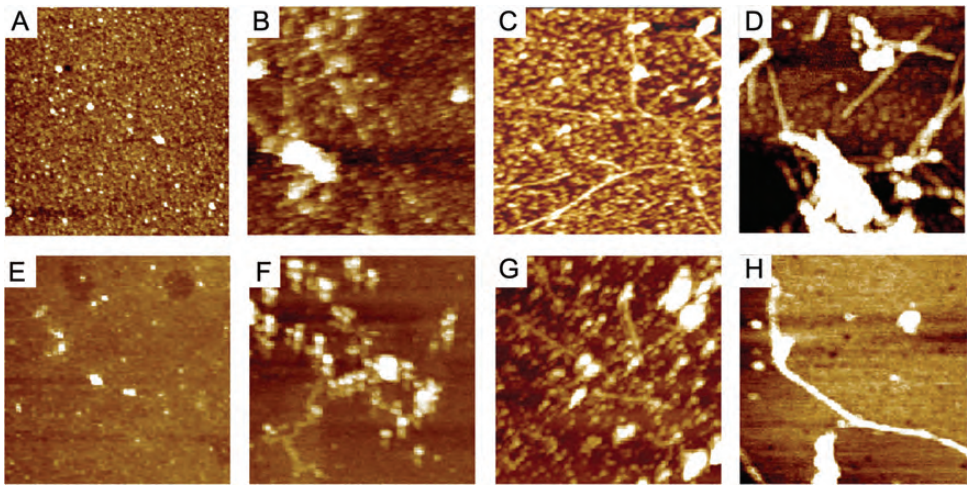

Figure 2 AFM images of Aβ solutions in the presence or absence of Cu^{2+} incubated at pH 4 and 25°C for different time Aβ solutions in the absence of Cu^{2+} for 0 h (A), 12 h (B), 48 h (C), and 168 h (D), as well as in the presence of Cu^{2+} for 0 h (E), 12 h (F), 48 h (G), and 168 h (H). The concentration of Aβ or Cu^{2+} was 25 μM. The scan area was 1 × 1 μm^2.

absence of Cu^{2+} at pH 4.0 were investigated by AFM. At the beginning of incubation, abundant Aβ oligomers formed in both solutions [**Fig. 2(A,E)**]. After 12 h incubation at 25°C, in sharp contrast to those observed at pH 5, a few protofibrils and amorphous aggregates appeared in both solutions [**Fig. 2(B,F)**]. As time elapsed, abundant long-linear fibrils accompanied with the appearance of abundant amorphous aggregates emerged in both solutions [**Fig. 2(D,H)**]. Comparison of these results with those at pH 5.0 revealed that lower pH of Aβ solution facilitated the formation of Aβ fibril morphology.

Temperature dependence of the aggregation rates and aggregates morphology

Temperature is an important factor influencing the aggregation rate and morphologies of Aβ aggregates [25,26]. To assess the temperature effect in the presence or absence of Cu^{2+}, the aggregation process of Aβ at 37°C (physiologically relevant temperature) was compared with that at 25°C. The time-lapse AFM images were collected from Cu^{2+}-free or Cu^{2+}-containing Aβ solutions (**Fig. 3**). There were abundant Aβ oligomers accompanied with a few amorphous aggregates at the beginning of incubation [**Fig. 3(A,E)**], implying that the process of aggregation was accelerated. After 12 h incubation, a few protofibrils appeared in Cu^{2+}-free solution [**Fig. 3(B)**], and abundant long-linear fibrils appeared as time elapsed [**Fig. 3(C)**]. In Cu^{2+}-containing solution, larger amorphous aggregates appeared [**Fig. 3(F)**] and a few protofibrils accompanied with amorphous aggregates appeared after 48 h incubation [**Fig. 3(G)**], then a mixture of fibrils and amorphous aggregates appeared in Cu^{2+}-containing solution when the incubation time reached up to

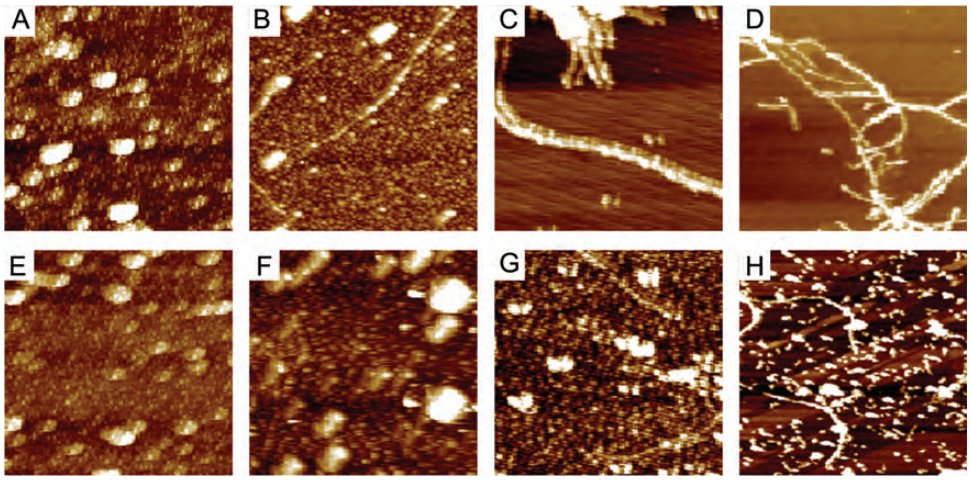

Figure 3 AFM images of Aβ solutions in the presence or absence of Cu^{2+} incubated at pH 4 and 37°C for different time Aβ solutions in the absence of Cu^{2+} for 0 h (A), 12 h (B), 48 h (C), and 168 h (D), as well as in the presence of Cu^{2+} for 0 h (E), 12 h (F), 48 h (G), and 168 h (H). The concentration of Aβ or Cu^{2+} was 25 μM. The scan area was 1 × 1 μm^2.

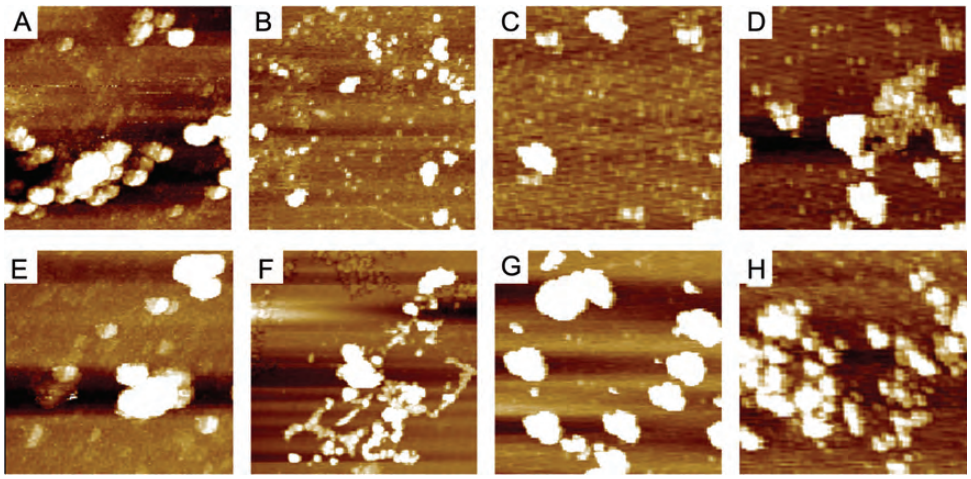

Figure 4 AFM images of Aβ solutions in the presence or absence of Cu^{2+} incubated at pH 5 and 37°C for different time Aβ solutions in the absence of Cu^{2+} for 0 h (A), 12 h (B), 48 h (C), and 168 h (D), as well as in the presence of Cu^{2+} for 0 h (E), 12 h (F), 48 h (G), and 168 h (H). The concentration of Aβ or Cu^{2+} was 25 μM. The scan area was 1 × 1 μm^2.

168 h [**Fig. 3(H)**]. However, only fibrils appeared in the Cu^{2+}-free solution with similar incubation [**Fig. 3(D)**]. When the molar ratio of Cu^{2+}/Aβ was increased to 2, the morphology of aggregates transformed from oligomers into amorphous aggregates directly (data not shown). The results confirmed that Cu^{2+} addition favors the formation of amorphous aggregates. Moreover, when compared with results at lower temperature (**Fig. 2**), the time required to form fibrils at 37°C was significantly decreased. These results indicated that the aggregation process of Aβ was accelerated at higher temperature.

Figure 4 showed the AFM images collected from Cu^{2+}-free and Cu^{2+}-containing Aβ solutions incubated at pH 5 and 37 °C for different time, respectively. In the Cu^{2+}-free solution, a few amorphous aggregates formed at the beginning of incubation [**Fig. 4(A)**]. After 12 h incubation, oligomers appeared together with a large amount of amorphous aggregates [**Fig. 4(B)**]. As time elapsed, larger amorphous aggregates formed in the Cu^{2+}-free solution, which was consistent with the previous results at 25°C [**Fig. 4(D)**]. In contrast, in the Cu^{2+}-containing solution, the aggregation pathway [**Fig. 4(E–H)**] was similar with that in Cu^{2+}-free solution [**Fig. 4(A–D)**], larger aggregates formed.

β-Sheet structure dependence of aggregation rates and morphology

Starting from random coil monomers, one Aβ molecule combines with one or more molecules by hydrogen bonding to form dimer or oligomers of β-sheet structures [27,28]. β-Sheet formation is a fast and pH-independent process [29]. In Zhou and coworker's research [20] on Aβ aggregates, it has been confirmed that both protofibrils/fibrils and

amorphous aggregates originate from the same partially folded β-sheet-containing intermediate. However, unlike the continuous growth of preformed protofibrils/fibrils upon incorporating monomers into fibrillar templates, the attachment of monomers and oligomers onto amorphous aggregates is random. Hence, the β-sheet contents were different in different aggregate morphologies. Therefore, ThT fluorescence could be used to monitor the formation of β-sheet during the aggregation process of Aβ.

Figure 5 showed the time-lapse ThT fluorescence intensity of Aβ under different environmental factors. The initial similar fluorescence intensities (24 ± 4) in all eight curves confirmed that the β-sheet formation was a really fast and pH-dependent process, which was consistent with results of the previous report [29]. As the incubation proceeded, the fluorescence intensity showed different tendencies under different environmental factors. At 25°C [**Fig. 5(A)**], a detectable increase in fluorescence intensity appeared only after 30 h incubation. However, at 37°C [**Fig. 5(B)**], the fluorescence intensity showed a sharp increase, reaching the highest value after 50 h incubation. These results confirmed that higher temperature promoted the formation of β-sheet structure, which accelerate fibril formation and amorphous aggregation. The ThT fluorescence only assesses fibril formation directly due to the specificity of ThT binds with amyloid β-sheets structures [22,30]. Nevertheless, the effect of high temperature on the formation of amorphous aggregation could not be investigated by ThT fluorescence. As time elapsed, a large amount of amorphous aggregates appeared and the fluorescence intensity started to decrease thereafter.

CD spectroscopy was used to monitor the secondary structure of Aβ. The techniques of ThT fluorescence and CD measure different aspects of amyloid aggregation. The ThT assay directly measures β-sheet structure only in fibril aggregation, and the CD techniques measures the formation of β-sheet structure irrespective of whether the aggregates are amorphous or fibrillar [30]. The CD spectrum at ~215 nm is characteristic of the β-sheet structure; the decreased ellipticity indicates the increased level of β-sheet conformation [22].

Figure 6 showed the ellipticity at 215 nm under different environmental factors. At the beginning of incubation, the secondary structures of Aβ were similar, which were all random coils (data not shown). As the incubation proceeded, the ellipticity curve indicated similar tendencies of β-sheet structure formation. Results confirmed that high temperature accelerated the aggregation rate, amorphous aggregates also contained β-sheet structure, and the presence of Cu^{2+} inhibited the formation of β-sheet structure.

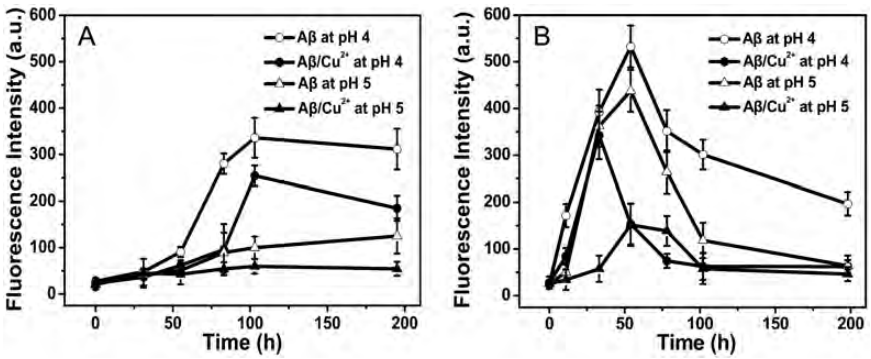

Figure 5 Time-lapse fluorescence intensity of Aβ solution measured at 485 nm in the absence or presence of Cu^{2+} The fluorescence intensity was measured at 25°C (A) or 37°C (B). The concentration of Aβ or Cu^{2+} was 25 μM.

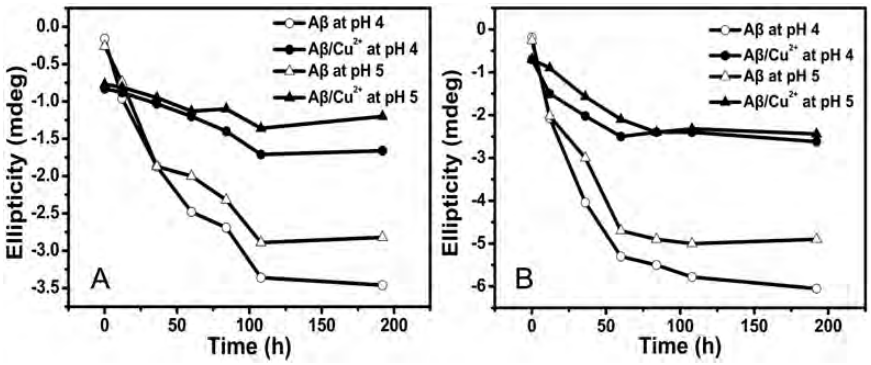

Figure 6 Time-lapse ellipticity of Aβ solution measured at 215 nm in the presence or absence of Cu^{2+} The ellipticity was measured at 25°C (A) and 37°C (B). The concentration of Aβ or Cu^{2+} was 25 μM.

Discussion

By monitoring the aggregation morphology and secondary structures of Aβ, it was discovered that the formation of Aβ fibril and the amorphous aggregation were two competitive processes governed by experimental factors such as pH, temperature, and Cu^{2+} binding. In previous papers, at neutral pH, Cu^{2+} binding results in the variation of charge and structure, which converts the morphology from fibril to amorphous aggregation [31,32], and the two competitive pathways diverged from same β-sheet-containing intermediates. However, in our research, it was clear that the Aβ aggregation process at low pH showed quite different feature from that at neutral pH. It could be summarized as: (i) lower pH favors the formation of fibrils aggregates; (ii) higher temperature accelerates the rate of fibril formation and amorphous aggregation; (iii) the binding of Cu^{2+} to Aβ inhibits the formation of β-sheet structure and favors amorphous aggregates. In addition to the effects of pH, temperature, and Cu^{2+} binding, other factors such as the local charge of ionizable amino acid residues, combined with conformation changes of Aβ, and the kinetics of β-sheet formation and stacking, should be taken into account.

The hydrophilic N-terminal (1–28) contains a high proportion of charged residues that are responsible for promoting or inhibiting aggregation rates in response to environmental variables. The hydrophobic C-terminal (29–42) is devoid of polar or charged amino acid residues, and almost exclusively oligomeric β-sheet structure in solution produce, unaffected by pH and temperature alterations [33]. At pH 4.5–6.6, the Glu and His side chains are all charged, β-sheet was formed and stabilized by the intermolecular ion-pairing interactions [34]. The β-sheet formation was noted as a rapid and pH-dependent process. The structure of Aβ dimers or partially folded oligomers was stabilized by hydrophobic side-chain interactions between the two β-sheets (i.e. β-sheet stacking) [35,36]. The emergence of the hairpin-structured β-sheet-stacked intermediate is a slow process [37]. Depending on experimental conditions, the β-sheet-containing dimers or partially folded oligomers, before developing into the hairpin structure, can coagulate to form amorphous aggregates. Competing with the main pathway to fibrils, the folding of Aβ molecules and the subsequent 'in-register' stacking of β-sheets are not kinetically favored [38].

As aforementioned, the pH and temperature affected the aggregation pathway. At pH 5.0 and 25°C, the morphology of Aβ aggregation was predominantly amorphous. At the same temperature but lower pH, abundant fibrils were observed. The production of amorphous aggregates was in common with the coalescence of colloidal particles, a process controlled by the electrostatics and intermolecular interaction such as the Van der Waals force. Analogous to the colloidal system, electrostatic repulsion between charged protein or peptide side chains creates a kinetic barrier to the coalescence of these molecules. In general, such barrier is not high and can be easily overcome by thermal energy. Thus, for proteins or peptides that are not highly charged, they will approach to each other and interact *via* intermolecular interactions, leading to amorphous aggregates by random combination. The diameter of amorphous aggregates formed at the beginning of the incubation under 37°C increased with the net surface charge of Aβ decreased (**Table 1**). Lowering the pH of the incubation solution increases the net positive charges on Aβ, as evidenced by the zeta potential decrease (**Table 1**). Such stability leaves enough time for the slow hairpin structure formation and the ordered β-sheet stacking [37,38].

An interesting observation was that the presence of Cu^{2+} in the incubation solution made the aggregation process to the direction of amorphous aggregate formation. An obvious decreased content of β-sheet structure and the unexpected negative shift on zeta potential values of Aβ in the presence of Cu^{2+} (**Table 1**) suggested that the Cu^{2+} binding to Aβ altered the Aβ structure. Since the initial β-sheet formation process (from random coil monomers to dimmer or oligomers of β-sheet structures) was fast [27–29,38], we hypothesized that complexation of Cu^{2+} with Aβ inhibited

Table 1 Zeta potential values of Aβ and Aβ/Cu^{2+} complex at different pH (T = *37*°C)

pH		Diameter of initial amorphous aggregates[a]	Major aggregate(s)[a]	Zeta potential
4.0	Aβ	80 ± 10 nm	Fibrils	12.80
	Aβ/Cu^{2+}	85 ± 10 nm	Amorphous aggregates, fibrils	7.28
	Aβ/2Cu^{2+}	88 ± 15 nm	Amorphous aggregates	6.56
5.0	Aβ	100 ± 5 nm	Amorphous aggregates	6.86
	Aβ/Cu^{2+}	130 ± 10 nm	Fibril, amorphous aggregates	5.81
	Aβ/2Cu^{2+}	170 ± 20 nm	Amorphous aggregates	4.71

[a]The statistics of diameter of initial amorphous aggregates and major aggregates were obtained from at least five regions (10 × 10 μm^2) of the sample surface.

the formation of hairpin structure and the subsequent stacking of β-sheet. This hypothesis could explain the detectable division of the fluorescence spectra after 12–20 h incubation.

The hydrophilic domain wrapped around the metal ion during metal ion complexation [39], and the Cu^{2+}/Aβ complex was wrapped by the positive charge at lower pH (e.g. 4, below the pI of Aβ 5.5). Compared with Aβ without Cu^{2+}, the surface charge on Cu^{2+}/Aβ is positively increased. Such a spatial rearrangement imposed greater steric hindrance to the orderly stacking of the β-sheets, and such a surface charge rearrangement may facilitate the intra- and intermolecular interaction between the hydrophilic and hydrophobic domains based on the Lys-28 $pK_a > 10$, Glu-22 pK_a 4.5, and Asp-23 pK_a 3.8 [34]. Moreover, low pH might disrupt the salt-bridge between Asp-23 and Lys-28, which made β-sheet structures unstable [40,41]. The same effect was extended to the β-sheet stacking process and the growth of oligomers into protofibrils. In the presence of Cu^{2+}, the final aggregation morphologies of Aβ changed from fibrils *via* a mixture of fibrils and amorphous aggregates to only amorphous aggregates (**Fig. 3**), which supported our conclusions. However, at pH 5, between the pI of Aβ and the pK_a of some pivotal amino acid residues (e.g. Glu-22, Asp-23, ~4), the aggregate morphology was confusing. With Cu^{2+}, only amorphous aggregates appeared, the participation of Cu^{2+} accelerated the rate of Aβ aggregation. These results remind us that the long-range effect of Cu^{2+} complexation on the charge of ionizable amino acid residues should be taken into account. The effect of Cu^{2+} was unimportant when the pH was far away from the pK_a of pivotal amino acid residues or the pI of Aβ. However, when the pH was close and between the pI of Aβ and the pK_a of amino acid residues, the long-range effect may be dominant due to its feasibility on changing electrostatic interaction between charged hydrophobic domain and some pivotal amino acid residues, which was important to the formation of β-sheet stacking process and the growth of oligomers into protofibrils.

The aggregation process of Aβ is considered to be a crucial step in AD development [42]. The physiological pH in the brain could decrease during the brain injury period, and the lower pH promotes the formation of toxic Aβ aggregates and the process of apoptosis [21]. Therefore, the effects of pH, Cu^{2+}, and temperature on the Aβ aggregation provide the information for the research of therapeutic strategies against AD.

In this work, the aggregation of $Aβ_{1-42}$ in the presence of Cu^{2+} under various experimental conditions (e.g. pH, temperature, and incubation time) was studied. Incubation temperature, pH, and the presence of Cu^{2+} in the Aβ solution were confirmed to alter the direction of aggregation (to fibrils or amorphous aggregates). The results of AFM indicated that the formation of fibrous morphology of Aβ is preferred at lower pH, but Cu^{2+} induced the presence of amorphous aggregates. The aggregation rate of Aβ increased with the elevation of temperature. These results were further confirmed by fluorescence spectroscopy and CD spectroscopy, it was found that the formation of β-sheet structure was inhibited by the Cu^{2+} binding to Aβ. We believe that the local charge state in hydrophilic domain of Aβ may play a dominant role in the aggregate morphology due to the strong steric hindrance. The research of Aβ aggregate morphology is valuable for the in-depth understanding of Aβ toxicity.

Funding

This work was supported by grants from the Postdoctoral Science Foundation of China, the National Natural Science Foundation of China (No. 20773165), the Scientific Research Fund of Hunan Provincial, the Science Foundation of Hunan Province, the Program for New Century Excellent Talents in University (No. NCET-07-0865), and the Postdoctoral Science Foundation of Central South University (No. P20-MD001824-01).

References

1 Roher AE, Lowenson JD, Clarke S, Woods AS, Cotter RJ, Gowing E and Ball MJ. β-Amyloid(1–42) is a major component of cerebrovascular amyloid deposits: Implications for the pathology of Alzheimer disease. Proc Natl Acad Sci USA 1993, 90: 10836–10840.

2 Masters CL, Simms G, Weinman NA, Multhaup G, McDonald BL and Beyreuther K. Amyloid plaque core protein in Alzheimer disease and Down syndrome. Proc Natl Acad Sci USA 1985, 82: 4245–4249.

3 Chimon S, Shaibat MA, Jones CR, Calero DC, Aizezi B and Ishii Y. Evidence of fibril-like beta-sheet structures in a neurotoxic amyloid intermediate of Alzheimer's beta-amyloid. Nat Struct Mol Biol 2007, 14: 1157–1164.

4 Tew DJ, Bottomley SP, Smith DP, Ciccotosto GD, Babon J, Hinds MG and Masters CL, *et al*. Stabilization of neurotoxic soluble β-sheet-rich conformations of the Alzheimer's disease amyloid-β peptide. Biophys J 2008, 94: 2752–2766.

5 Dai X, Sun Y and Jiang Z. Cu(II) potentiation of Alzheimer Aβ1–40 cytotoxicity and transition on its secondary structure. Acta Biochim Biophys Sin 2006, 38: 765–772.

6 Barrow CJ and Zagorski MG. Solution structures of beta peptide and its constituent fragments-relation to amyloid deposition. Science 1991, 253: 179–182.

7 Burdick D, Soreghan B, Kwon M, Kosmoski J, Knauer M, Henschen A and Yates J, *et al*. Assembly and aggregation properties of synthetic Alzheimers A4/beta amyloid peptide analogs. J Biol Chem 1992, 267: 546–554.

8 Snyder SW, Ladror US, Wade WS, Wang GT, Barrett LW, Matayoshi ED and Huffaker HJ, *et al*. Amyloid-β aggregation-selective-inhibition of aggregation in mixtures of amyloid with different chain lengths. Biophys J 1994, 67: 1216–1228.

9 Yoshiike Y, Akagi T and Takashima A. Surface structure of amyloid-β fibrils contributes to cytotoxicity. Biochemistry 2007, 46: 9805–9812.

10 Dai X, Sun Y, Gao Z and Jiang Z. Copper enhances amyloid-beta peptide neurotoxicity and non beta-aggregation: a series of experiments conducted upon copper-bound and copper-free amyloid-beta peptide. J Mol Neurosci 2010, 41: 66–73.

11 Faller P and Hureau C. Bioinorganic chemistry of copper and zinc ions coordinated to amyloid-β peptide. Dalton Trans 2009, 1080–1094.

12 Kraig RP, Pulsinelli WA and Plum F. Heterogeneous distribution of hydrogen and bicarbonate ions during complete brain ischemia. Prog Brain Res 1985, 63: 155–166.

13 Su Y and Chang PT. Acidic pH promotes the formation of toxic fibrils from beta-amyloid peptide. Brain Res 2001, 893: 287–291.

14 Perálvarez-Marín A, Barth A and Gräslund A. Time-resolved infrared spectroscopy of pH-induced aggregation of the Alzheimer Aβ1–28 peptide. J Mol Biol 2008, 379: 589–596.

15 Tomaselli S, Esposito V, Vangone P, van Nuland NAJ, Bonvin AMJJ, Guerrini R and Tancredi T, *et al*. The α-to-β conformational transition of Alzheimer's Aβ(1–42) peptide in aqueous media is reversible: a step by step conformational analysis suggests the location of β conformation seeding. Chembiochem 2006, 7: 257–267.

16 Atwood CS, Moir RD, Huang X, Scarpa RC, Bacarra NME, Romano DM and Hartshorn MA, *et al*. Dramatic aggregation of Alzheimer Aβ by Cu(II) is induced by conditions representing physiological acidosis. J Biol Chem 1998, 273: 12817–12826.

17 Yoshiike Y, Tanemura K, Murayama O, Akagi T, Murayama M, Sato S and Sun X, *et al*. New insights on how metals disrupt amyloid β-aggregation and their effects on amyloid-β cytotoxicity. J Biol Chem 2001, 276: 32293–32299.

18 Raman B, Ban T, Yamaguchi K, Sakai M, Kawai T, Naiki H and Goto Y. Metal ion-dependent effects of clioquinol on the fibril growth of an amyloid β peptide. J Biol Chem 2005, 280: 16157–16162.

19 Rózga M, Kłoniecki M, Dadlez M and Bal W. A direct determination of the dissociation constant for the Cu(II) complex of amyloid β 1–40 peptide. Chem Res Toxicol 2010, 23: 336–340.

20 Jiang D, Rauda I, Han S, Chen S and Zhou F. Aggregation pathways of the Amyloid β(1–42) peptide depend on its colloidal stability and ordered β-sheet stacking. Langmuir 2012, 28: 12711–12721.

21 Bin Y, Chen S and Xiang J. pH-dependent kinetics of copper ions binding to amyloid-β peptide. J Inorg Biochem 2013, 119: 21–27.

22 Jun S, Gillespie JR, Shin B and Saxena S. The second Cu(II)-binding site in a proton-rich environment interferes with the aggregation of amyloid-β(1−40) into amyloid fibrils. Biochemistry 2009, 48: 10724–10732.

23 Hartley DM, Walsh DM, Ye CP, Diehl T, Vasquez S, Vassilev PM and Teplow DB, *et al*. Protofibrillar intermediates of amyloid β-protein induce acute electrophysiological changes and progressive neurotoxicity in cortical neurons. J Neurosci 1999, 19: 8876–8884.

24 Wood SJ, Maleeff B, Hart T and Wetzel R. Physical, morphological and functional differences between pH 5.8 and 7.4 aggregates of the Alzheimer's amyloid peptide Aβ. J Mol Biol 1996, 256: 870–877.

25 Gursky O and Aleshkov S. Temperature-dependent β-sheet formation in β-amyloid Aβ1–40 peptide in water: Uncoupling β-structure folding from aggregation. BBA-Protein Struct M 2000, 1476: 93–102.

26 Lin S, Chu H and Wei Y. Secondary conformations and temperature effect on structural transformation of amyloid beta (1–28), (1–40) and (1–42) peptides. J Biomol Struct Dyn 2003, 20: 595–601.

27 Garzon-Rodriguez W, Sepulveda-Becerra M, Milton S and Glabe CG. Soluble amyloid Aβ(1–40) exists as a stable dimer at low concentrations. J Biol Chem 1997, 272: 21037–21044.

28 Hilbich C, Kisters-Woike B, Reed J, Masters CL and Beyreuther K. Aggregation and secondary structure of synthetic amyloid βA4 peptides of Alzheimer's disease. J Mol Biol 1991, 218: 149–163.

29 Sivaraman T, Kumar TKS, Chang DK, Lin WY and Yu C. Events in the kinetic folding pathway of a small, all β-sheet protein. J Biol Chem 1998, 273: 10181–10189.

30 Benseny-Cases N, Cócera M and Cladera J. Conversion of non-fibrillar β-sheet oligomers into amyloid fibrils in Alzheimer's disease amyloid peptide aggregation. Biochem Biophys Res Commun 2007, 361: 916–921.

31 Zou J, Kajita K and Sugimoto N. Cu^{2+} inhibits the aggregation of amyloid β-peptide(1–42) in vitro. Angew Chem Int Ed 2001, 40: 2274–2277.

32 Ciccotosto GD, Tew DJ, Fodero-Tavoletti MT, Johanssen T, Masters CL, Barnham KJ and Cappai R. Concentration dependent Cu^{2+} induced aggregation and dityrosine formation of the Alzheimer's disease Amyloid-β peptide. Biochemistry 2007, 46: 2881–2891.

33 Barrow CJ, Yasuda A, Kenny PTM and Zagorski MG. Solution conformations and aggregational properties of synthetic amyloid β-peptides of Alzheimer's disease: analysis of circular dichroism spectra. J Mol Biol 1992, 225: 1075–1093.

34 Ma K, Clancy EL, Zhang Y, Ray DG, Wollenberg K and Zagorski MG. Residue-specific pKa measurements of the β-peptide and mechanism of pH-induced amyloid formation. J Am Chem Soc 1999, 121: 8698–8706.

35 Petkova AT, Ishii Y, Balbach JJ, Antzutkin ON, Leapman RD, Delaglio F and Tycko R. A structural model for Alzheimer's β-amyloid fibrils based on experimental constraints from solid state NMR. Proc Natl Acad Sci USA 2002, 99: 16742–16747.

36 Lührs T, Ritter C, Adrian M, Riek-Loher D, Bohrmann B, Döbeli H and Schubert D, *et al*. 3D structure of Alzheimer's amyloid-β(1–42) fibrils. Proc Natl Acad Sci USA 2005, 102: 17342–17347.

37 Sciarretta KL, Gordon DJ, Petkova AT, Tycko R and Meredith SC. Aβ40-lactam(D23/K28) models a conformation highly favorable for nucleation of amyloid. Biochemistry 2005, 44: 6003–6014.

38 Nelson R, Sawaya MR, Balbirnie M, Madsen AO, Riekel C, Grothe R and Eisenberg D. Structure of the cross-β spine of amyloid-like fibrils. Nature 2005, 435: 773–778.

39 DeMarco ML and Daggett V. Molecular mechanism for low pH triggered misfolding of the human prion protein. Biochemistry 2007, 46: 3045–3054.

40 Resende R, Ferreiro E, Pereira C and Resende de Oliveira C. Neurotoxic effect of oligomeric and fibrillar species of amyloid-beta peptide 1–42: Involvement of endo-plasmic reticulum calcium release in oligomer-induced cell death. Neuroscience 2008, 155: 725–737.

41 Syme CD, Nadal RC, Rigby SEJ and Viles JH. Copper binding to the amyloid-β (Aβ) peptide associated with Alzheimer's disease. J Biol Chem 2004, 279: 18169–18177.

42 Fraser PE, McLachlan DR, Surewicz WK, Mizzen CA, Snow AD, Nguyen JT and Kirschner DA. Conformation and fibrillogenesis of Alzheimer Aβ peptides with selected substitution of charged residues. J Mol Biol 1994, 244: 64–73.